Co-published by
Institute of Fluid-Flow Machinery
Polish Academy of Sciences
Committee on Thermodynamics and Combustion
Polish Academy of Sciences

Copyright©2024 by the Authors under licence CC BY 4.0

http://www.imp.gda.pl/archives-of-thermodynamics/

Integrating PEM fuel cell control with building heating systems: A comprehensive thermal and control model analysis

Robert Matysko[a*]

[a]Institute of Fluid-Flow Machinery, Polish Academy of Sciences, Fiszera 14 st., Gdańsk 80-231, Poland
*Corresponding author email: matyskor@imp.gda.pl

Received: 24.08.2023; revised: 17.02.2024; accepted: 10.05.2024

Abstract

In the paper, a model of a heated building using a PEM (proton exchange membrane) fuel cell is presented. This work introduces a novel and more comprehensive depiction of the thermal processes occurring within a fuel cell under transient conditions. The developed PEM fuel cell model was synergistically incorporated with a thermodynamic model of a building. The resulting mathematical framework provides insights into the building's performance concerning fluctuating ambient temperatures and the heating system powered by the PEM cell. The developed mathematical model delineates the interplay between the building's thermodynamics and the fuel cell in the context of the devised heating control system featuring an indirect heat distribution mechanism.

Keywords: PEM fuel cell; Thermal dynamics; Building heating system; Transient model; Waste heat recovery

Vol. 45(2024), No. 3, 209–219; doi: 10.24425/ather.2024.151232

Cite this manuscript as: Matysko, R. Integrating PEM fuel cell control with building heating systems: A comprehensive thermal and control model analysis. *Archives of Thermodynamics*, 45(3), 209–219.

1. Introduction

This paper explains the control process of a PEM cell concerning the utilisation of waste heat within buildings. The supply of fuel and oxidant to the fuel cell is facilitated through a valve system actuated by stepper motors. Given the proportional demand for reaction substrates, it becomes feasible to employ a single regulator with suitably chosen stepper motor-driven valves to energize the PEM cell. The second regulator finds application in the PEM cell's cooling system – this configuration could also function as a means to distribute heat to the building's rooms. Based on existing literature, this paper introduces a new continuous control system employing a singular SIMO (Single Input, Multiple Output) type regulator for the PEM cell. Furthermore, the article presents an innovative fuel cell temperature control system, that exploits the potential for waste heat recovery and subsequent utilization for heating purposes. A novel mathematical model, encompassing the fuel cell's temperature control process to meet heat demands within buildings is proposed.

Nomenclature

A – heat transfer surface, channel cross-section normal to flow, m^2
c – specific heat, J/(kg K)
c_i – molar specific heat (i = H_2, O_2, H_2O), J/(mol K)
$e(t)$ – control deviation
G – Laplace transform transfer function
h – specific enthalpy, J/kg
H – enthalpy of formation, J/mol
I – electric current, A
k – overall heat transfer coefficient, W/(m^2K)
m – mass, kg
$\dot{n}$ – molar flow, mol/s
P – electrical power, W
$\dot{Q}$ – heat flux, W
s – Laplace operator
S – channel cross-section normal to flow, m^2
t – time, s
T – temperature, K
U – voltage, V
w – flow velocity, m/s
x – flow path between inlet and outlet of the heat exchanger, m

Greek symbols

ρ – density, kg/m^3

Subscripts and Superscripts

b – room under study
bw – solid wall (without glazing) between the room under study and the external environment
d – differentiating (in reference to gain)
gd – ground
h – heater
i – integrating (in reference to gain)
in – inlet
k_1 – corridor
k_2 – corridor
l – saturated liquid water
net – total heat balance
o – external environment
out – outlet
p – proportional (in reference to gain)
p_n – adjacent rooms (n = 1,…,5)
s – ceiling, saturated water vapour
set – controller setting
str – acquired stream
uj – latent and sensible heat
w – glazed wall between the room under study and the external environment
win – inlet water
chem – chemical reaction
wout – outlet water

Abbreviations and Acronyms

PEM – proton exchange membrane
PID – proportional-integral-derivative

Over the past century, a variety of power systems dedicated to energy conversion has emerged – extending beyond the confines of the Rankine vapour cycle. Among these systems, fuel cells stand out as prominent examples. Fuel cells are predominantly associated with energy conversion mechanisms rooted in hydrogen oxidation without combustion. The fuel cell landscape encompasses a variety of types, including Solid Oxide Fuel Cells (SOFC), Proton Exchange Membrane Fuel Cells (PEMFCs), Alkaline Fuel Cells (AFC), and Phosphoric Acid Fuel Cells (PAFC), among others. Fuel cells readily lend themselves to mathematical modelling concerning the thermodynamic processes involved. The control process of PEM fuel cells was described by Nehrir and Wang [1]. Their study offers a relatively comprehensive model of the PEM fuel cell, and while the heat exchange with the surroundings is somewhat simplified, the mathematical description precludes the estimation of temperature elevation in the fuel cell's coolant.

The current body of literature not only encompasses transient models for PEM cells [1] but also includes more intricate elucidations of the processes occurring in these cells. Notably, certain papers offer more detailed insights into phenomena like two-phase flow [2]. However, these models are predominantly tailored to PEM cells operating under steady-state conditions. Consequently, they are inadequate for simulating the behaviour of PEM cells during start-up, shutdown, or when subjected to varying heat loads over time – scenarios that include heat recovery, a factor that directly affects the energy efficiency of fuel cells.

In the Abdin et al. study [3], a transient model was meticulously developed to delineate the chemical and electrochemical processes in a fuel cell. Although somewhat lacking precision in explaining thermal processes, it proved useful in understanding PEM fuel cell dynamics from an electro-technical perspective. Taner [4] characterised electrical parameters related to substrate pressure in the fuel cell, employing a steady-state PEM cell model to determine cell exergy He evaluated a PEM fuel cell's performance based on operating pressure and voltage parameters, finding energy and exergy efficiencies of 47.6% and 50.4%, respectively, and highlighting wastewater management's importance in fuel cell lifespan. In another study [5], Taner compared traditional PEM fuel cell systems with nano-designed versions, demonstrating significantly higher energy (72.4%) and exergy (85.22%) efficiencies in the latter, and suggesting that pressure and flow rate optimizations can greatly enhance thermodynamic efficiency. Naqvi et al. [6] conducted a techno-economic and enviro-economic analysis of hydrogen production using an optimised alkaline electrolyser. The authors developed a prototype that efficiently produced oxyhydrogen gas, evidencing economic feasibility with a favourable payback period. Lastly, paper [7] introduces an innovative PEM electrolyser prototype for hydrogen generation, featuring Cr-C coated SS304 bipolar plates and a specialized chemical mixture, achieving a production rate of 6 m³/h and an economically advantageous payback period, showcasing efficiency and cost-effectiveness.

In the context of the study of Sudarshan and Dhananjay [8], PEM cell dynamics is characterised by assuming equal partial

pressures for hydrogen and oxygen. Notably, the model's implementation in SIMULINK software falls short of accommodating temperature variations in the PEM fuel cell's cooling medium. A detailed description of physical models situating the PEM cell in a three-dimensional space under steady-state conditions is presented in the study of Mingruo et al. [9]. Herein, the authors presented the PEM cell voltage/current characteristic observed under steady conditions.

Moving forward, Ziogou et al. [10] not only modelled the PEM cell but also confirmed the model predictions through experimental validation, focusing on the cell's electrodynamic attributes. The work [11] details PEM cell test outcomes while incorporating PI and Fuzzy Logic regulators for control. Describing an alternative configuration, Waseem and Ghait [12] outlined a PEM cell model wherein substrate production was driven by PV cells. A distinct model, as presented in [13], explicates the dynamics of proton diffusive transport through the PEM cell's membrane.

Given that the primary application of PEM fuel cells revolves around electricity generation, the prevailing literature predominantly emphasizes models aimed at calculating electricity and voltage parameters. Notably, software tools like Matlab/Simulink, particularly within the Simscape™ Electrical™ toolbox [14], have integrated models of diverse fuel cell types (e.g., PEM, SOFC, AFC), primarily focused on configuring electricity and voltage attributes. Regrettably, the models integrated within this software fail to account for the thermal characteristics of the cell arising from heat dissipation into the surroundings and the cell's interaction with heating systems.

Within the realm of literature, the examination of building dynamics finds expression through the utilisation of the thermoelectric analogy, a concept comprehensively expounded upon in studies [15,16]. In [17], fundamental principles related to heat management and the quantification of energy balances within buildings are elucidated, alongside the presentation of guidelines for constructing such energy balances. Mathematically detailing heat flow between heated and unheated spaces is a relatively straightforward task. Nevertheless, due to the reliance on factors such as wall materials, inter-room thermal processes, and ambient thermal conditions, the actual process of formulating equations governing heat transfer becomes protracted and intricate.

Windows significantly influence building energy use and thermal comfort. While many models exist for assessing indoor thermal comfort, the effect of solar radiation is often neglected. Song et al. [18] applied the SMRT (simplified mean radiant temperature)-air temperature deviation method to evaluate solar radiation's impact on indoor comfort during the initial design phase. Focusing on office buildings in various orientations and climates, the findings indicate a more pronounced impact of solar radiation in colder climates, especially through east and west-facing windows. Adjusting the Solar Heat Gain Coefficient (SHGC) of windows could reduce discomfort by over 86% across all climates, aiding designers in enhancing indoor thermal comfort. Wonorahardjo et al. [19] explored how various façade systems impact thermal comfort and Urban Heat Island (UHI) effects. Their study involved outdoor field measurements on materials like brick, concrete, low-E (low-emissivity) glass, and Aluminium Composite Panel (ACP), focusing on solar exposure effects on façade surface temperatures. Additional lab experiments under simulated solar exposure assessed the thermal behaviour of these materials. Findings showed that brick walls stored and emitted heat, affecting both indoor and outdoor temperatures. Adding ACP to brick walls significantly lowered indoor temperatures but may contribute to UHI. Insulation materials like newspaper and corn husk mats were effective in reducing indoor temperatures during the heating period but slightly increased outdoor temperatures. The study underscored the importance of considering both indoor and outdoor temperatures in building design for thermal comfort and UHI mitigation.

In HVAC system design, balancing user comfort and energy consumption often leads to a conflict, requiring Pareto-optimal controls. While indoor air temperature is a common control parameter, it does not always accurately capture perceived thermal comfort due to sensor placement. Computational fluid dynamics (CFD) can help develop more effective control strategies [20]. A comparative study between PMV (predicted mean vote)-based thermal comfort control and traditional temperature-based control in a sunlit office room showed that an iterative approach for adjusting air supply flow can better meet ISO 7730 comfort standards. CFD simulations compared air temperature distribution and ventilation effectiveness for both strategies, analysing thermal indices and energy savings. The PMV-based control not only enhanced thermal comfort in the glazed office but also reduced energy use by 1.6% daily.

A numerical study in research [21] examines the energy consumption of bedroom task/ambient air conditioning (TAC) across different climate zones, focusing on a PMV-based control strategy for night-time energy use. Two traditional operating modes were analysed: variable supply air temperature (VAT) and variable supply air flow rate (VAF). Results showed that VAT mode reduces energy consumption significantly more than VAF, with savings of at least 10% in Beijing, 19% in Shanghai, and 18% in Guangzhou. An optimized mode, VFT-LowE, which combines variable flow rate and temperature, was found to save up to 6.5% more energy than VAT mode in Guangzhou. The study also highlighted that the highest energy-saving potential is observed in warmer climates, reaching up to 403 kJ per night in Beijing and around 1100 kJ in Shanghai and Guangzhou. The findings suggested the effectiveness of optimized TAC operation modes in reducing energy consumption, particularly in hotter climates.

Buyak et al., in the previous work [23], based on experimental analysis demonstrated that enhancing thermal insulation to Swedish standards and adopting intermittent heating can significantly reduce energy consumption. However, they also highlighted the need for additional electric heating during transition periods to maintain comfort, potentially increasing energy consumption. The results of the research might be useful for identifying the thermal characteristics of a building, even though they did not include a mathematical description of the building that could be used to simulate its thermal dynamics. A mathematical model of such a building is presented in the present work.

2. Mathematical modelling of a building heated by a PEM cell

This section provides an in-depth analysis of a mathematical model that comprehensively covers various facets of the PEM cell control system. Specifically, the focus lies on both electricity generation and the recovery process of waste heat. The model incorporates the utilization of logarithmic temperature differences as output parameters, serving as a metric for assessing the stability of the PEM cell. Furthermore, the chapter introduces a mathematical model adapted to a building with a PEM cell, utilized primarily for heating purposes.

The thermal dynamics of room, subject to temperature fluctuations, is influenced by a myriad of factors. These factors encompass solar radiation exposure within the room, the operation of electrical and heating appliances, occupancy levels, the effectiveness of the ventilation system, as well as heat exchange with the external environment and the ground.

The ambient temperature within a designated room is an outcome of achieving a balance between heat influx and dissipation. When heat dissipation surpasses influx, a gradual temperature decrease is observed. Conversely, heat influx higher than dissipation leads to temperature elevation. The equilibrium between these heat factors holds pivotal importance in maintaining the desired room temperature. Notably, such equilibrium is predominantly attainable under stable operating conditions, a criterion upon which heat-providing systems are designed. Real-world scenarios, however, entail dynamic heat influx and dissipation, resulting in fluctuating and occasionally uneven heat distribution across various rooms.

Accurately quantifying heat flow through the walls delineating the volume of a heated room proves to be a complex task. This section presents a mathematical model that determines the diurnal oscillations of the temperature (T_b) in the analysed room. These fluctuations are driven by the introduction of warm water sourced from the PEM fuel cell. The spatial proximity of the room to heated chambers (T_{p1}, T_{p2}, T_{p3}, T_{p4}, T_{p5}) and unheated halls (T_{k1} and T_{k2}) establishes boundaries with the external environment, potentially extending to the ground surface based on geographical nuances (Fig. 1).

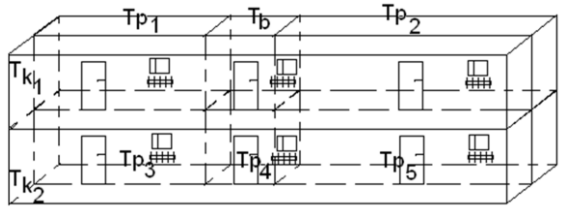

Fig. 1. Diagram depicting the configuration of the simulated rooms.

The computations were performed to determine the temperature changes that occur due to the difference between the heat demand (losses) and the heat supplied (gains) from the PEM fuel cell.

Figure 2 depicts a negative feedback loop where the controlled variables of molar hydrogen expenditure (nH_2) and molar oxygen expenditure (nO_2) depend on the temperature T3 of the water (H_2O) exiting the fuel cell and PID (proportional-integral-derivative) controller settings.

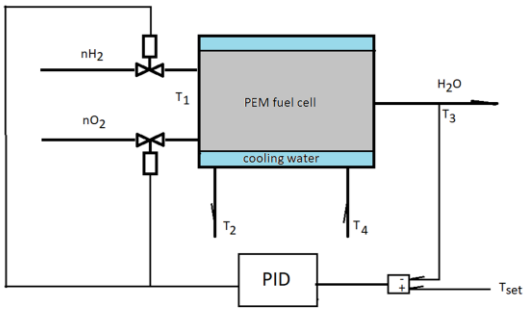

Fig. 2. PID control system for the PEM fuel cell.

The mathematical model of the room operates under the following assumptions and simplifications [23]:

1) It depicts daily temperature fluctuations during winter.
2) Heat gains from solar radiation and electrical appliances have been excluded.
3) Changes in humidity, as well as gains and losses through the ventilation system, have not been considered.
4) The anticipated sinusoidal temperature changes within the room are linked to the controller.
5) The ambient temperature is represented by a signal that linearly increases and decreases.
6) Heat transfer coefficients are assumed to be the same for walls adjacent to external surroundings and unheated rooms.

While in operation, the PEM fuel cell (Fig. 2) generates electricity and concurrently produces thermal energy. The model applied to the fuel cell is based on the following assumptions [1]:

1) It operates transiently.
2) The fuel cell's characterisation employs spatial parameters.
3) Control of the modelled fuel cell is based on the logarithmic temperature difference between the cell and the cooling water. The temperature of cooling water is set at a level that optimizes its applicability for heating purposes.
4) The entire heat generated during the reaction is effectively transferred to the heating system.
5) Fluid flow within the fuel cell is turbulent, characterised by a Reynolds number (Re) exceeding 10000.
6) The discrepancy in enthalpy during the phase transition between steam and water is determined by a value dependent on the saturation pressure of the two-phase mixture.

The mathematical model for the building includes the equations describing the temperature changes over the time within: (i) the analysed room, (ii) room $p1$, (ii) room $p2$, (iii) room $p3$, (iv) room $p4$, and (v) hall $k1$, and (vi) hall $k2$, respectively:

$$\frac{dT_b}{dt}m_b c_b = A_{b-p1}k_{b-p1}(T_{p1}-T_b) + A_{b-p2}k_{b-p2}(T_{p2}-T_b) + A_{b-p3}k_{b-p3}(T_{p3}-T_b) + A_{b-p4}k_{b-p4}(T_{p4}-T_b) + \\ +A_{b-p5}k_{b-p5}(T_{p5}-T_b) + A_{b-s}k_{b-s}(T_o-T_b) + A_{b-w}k_{b-w}(T_o-T_b) + A_{b-k1}k_{b-k1}(T_{k1}-T_b) + \\ +A_{b-k2}k_{b-k2}(T_{k2}-T_b) + A_{h-pb}k_{h-pb}(T_h-T_{pb}), \quad (1)$$

$$\frac{dT_{p1}}{dt}m_{p1}c_{p1} = A_{b-p1}k_{b-p1}(T_b-T_{p1}) + A_{k1-p1}k_{k1-p1}(T_{k1}-T_{p1}) + A_{k2-p1}k_{k2-p1}(T_{k2}-T_{p1}) + \\ +A_{p1-p3}k_{p1-p3}(T_{p3}-T_{p1}) + A_{p1-p4}k_{p1-p4}(T_{p4}-T_{p1}) + A_{p1-w}k_{p1-w}(T_o-T_{p1}) + \\ +A_{p1-bw}k_{p1-bw}(T_o-T_{p1}) + A_{p1-s}k_{p1-s}(T_o-T_{p1}) + A_{h-p1}k_{h-p1}(T_h-T_{p1}), \quad (2)$$

$$\frac{dT_{p2}}{dt}m_{p2}c_{p2} = A_{b-p2}k_{b-p2}(T_b-T_{p2}) + A_{k1-p2}k_{k1-p2}(T_{k1}-T_{p2}) + A_{k2-p2}k_{k2-p2}(T_{k2}-T_{p2}) + \\ +A_{p4-p2}k_{p4-p2}(T_{p4}-T_{p2}) + A_{p5-p2}k_{p5-p2}(T_{p5}-T_{p2}) + A_{p2-w}k_{p2-w}(T_o-T_{p2}) + \\ +A_{p2-bw}k_{p2-bw}(T_o-T_{p2}) + A_{p2-s}k_{p2-s}(T_o-T_{p2}) + A_{h-p2}k_{h-p2}(T_h-T_{p2}) \quad (3)$$

$$\frac{dT_{p3}}{dt}m_{p3}c_{p3} = A_{b-p3}k_{b-p3}(T_b-T_{p3}) + A_{k1-p3}k_{k1-p3}(T_{k1}-T_{p3}) + A_{k2-p3}k_{k2-p3}(T_{k2}-T_{p3}) + \\ +A_{p4-p3}k_{p4-p3}(T_{p4}-T_{p3}) + A_{p3-w}k_{p3-w}(T_o-T_{p3}) + A_{p3-bw}k_{p3-bw}(T_o-T_{p3}) + \\ +A_{p3-gd}k_{p2-gd}(T_{gd}-T_{p3}) + A_{h-p3}k_{h-p3}(T_h-T_{p3}), \quad (4)$$

$$\frac{dT_{p4}}{dt}m_{p4}c_{p4} = A_{b-p4}k_{b-p4}(T_b-T_{p4}) + A_{k1-p4}k_{k1-p4}(T_{k1}-T_{p4}) + A_{k2-p4}k_{k2-p4}(T_{k2}-T_{p4}) + \\ +A_{p4-w}k_{p4-w}(T_o-T_{p4}) + A_{p4-gd}k_{p4-gd}(T_{gd}-T_{p4}) + A_{h-p4}k_{h-p4}(T_h-T_{p4}) + \\ +A_{p1-p4}k_{p1-p4}(T_{p1}-T_{p4}) + A_{p2-p4}k_{p2p4}(T_{p2}-T_{p4}) + A_{p3-p4}k_{p3-p4}(T_{p3}-T_{p4}) + A_{p5-p4}k_{p5-p4}(T_{p5}-T_{p4}), \quad (5)$$

$$\frac{dT_{p5}}{dt}m_{p5}c_{p5} = A_{b-p5}k_{b-p5}(T_b-T_{p5}) + A_{k1-p5}k_{k1-p5}(T_{k1}-T_{p5}) + A_{k2-p5}k_{k2-p5}(T_{k2}-T_{p5}) + \\ +A_{p5-w}k_{p5-w}(T_o-T_{p5}) + A_{p5-bw}k_{p5-bw}(T_o-T_{p5}) + A_{p5-gd}k_{p5-gd}(T_{gr}-T_{p5}) + A_{h-p5}k_{h-p5}(T_h-T_{p5}) + \\ +A_{p1-p4}k_{p1-p4}(T_{p1}-T_{p4}) + A_{p2-p5}k_{p2-p5}(T_{p2}-T_{p5}) + A_{p5-p4}k_{p5-p4}(T_{p4}-T_{p5}), \quad (6)$$

$$\frac{dT_{k1}}{dt}m_{k1}c_{k1} = A_{b-k1}k_{b-k1}(T_b-T_{k1}) + A_{k1-p1}k_{k1-p1}(T_{p1}-T_{k1}) + A_{k1-p2}k_{k1-p2}(T_{p2}-T_{k1}) + \\ +A_{k1-p3}k_{k1-p3}(T_{p3}-T_{k1}) + A_{k1-p4}k_{k1-p4}(T_{p4}-T_{k1}) + A_{k1-p5}k_{k1-p5}(T_{p5}-T_{k1}) + \\ +A_{k1-k2}k_{k1-k2}(T_{k2}-T_{k1}) + 2\cdot A_{k1-w}k_{k1-w}(T_o-T_{k1}) + A_{k1-s}k_{k1-s}(T_s-T_{k1}), \quad (7)$$

$$\frac{dT_{k2}}{dt}m_{k2}c_{k2} = A_{b-k2}k_{b-k2}(T_b-T_{k2}) + A_{k2-p1}k_{k2-p1}(T_{p1}-T_{k2}) + A_{k2-p2}k_{k2-p2}(T_{p2}-T_{k2}) + \\ +A_{k2-p3}k_{k2-p3}(T_{p3}-T_{k2}) + A_{k2-p4}k_{k2-p4}(T_{p4}-T_{k2}) + A_{k2-p5}k_{k2-p5}(T_{p5}-T_{k2}) + \\ +A_{k1-k2}k_{k1-k2}(T_{k1}-T_{k2}) + 2\cdot A_{k2-w}k_{k2-w}(T_o-T_{k2}) + A_{k2-gd}k_{k2-gd}(T_{gd}-T_{k2}), \quad (8)$$

where: m – mass, T – temperature, c – specific heat, A – heat transfer surface area, channel cross-section normal to flow, k – overall heat transfer coefficient, t – time. In Eqs. (1)–(8), the subscripts refer to the following, respectively: $k1$, $k2$ – corridor, gd – ground, h – heater; b – room under study, bw – solid wall (without glazing) between the room under study and the external environment, o – external environment; $p1,\ldots,p5$ – adjacent rooms, w – glazed wall between the room under study and the external environment.

Heating for the building is obtained by utilising water from the fuel cell's cooling system, which is controlled by a PID controller. The mathematical representation of both the control system for the hot water supply and the controller is presented below.

The heating process is described by the equation:

$$\rho c S\frac{dT_h}{dt} = \rho w c S\frac{T_{win,h}-T_h}{\Delta x/_2} - \rho w c S\frac{T_h-T_{wout,h}}{\Delta x/_2} - \\ -A_h k_h \frac{(T_{win,h}-T_h)-(T_{wout,h}-T_h)}{\ln\left(\frac{(T_{win,h}-T_h)}{(T_{wout,h}-T_h)}\right)}, \quad (9)$$

where: S – pipeline cross-section, ρ – density, x – flow path between inlet and outlet of the heat exchanger, w – flow velocity, *win* – inlet water; *wout* – outlet water.

The process of regulation of flow through the heat exchanger is determined by the correlation:

$$G_{PID}(s) = \left(K_p + \frac{K_i}{s} + K_d s\right) = \\ = k_p\left(e(t) + \frac{1}{T_i}\int_0^t e(t)dt + T_d\frac{de(t)}{dt}\right), \quad (10)$$

$$e(t) = (w_{set} - w), \quad (11)$$

$$K_p = k_p,\ K_i = \frac{k_p}{T_i},\ K_d = k_d T_d, \quad (12)$$

where: $e(t)$ – control deviation; s – Laplace operator, k – gain of the PID controller; T – time constant. The respective subscripts are: p – proportional; d – differentiation; i – integration; *set* – controller setting.

The PEM cell model addresses transient conditions; nonetheless, this model takes into account heat exchange with the

surroundings, phase transitions, and chemical reactions occurring within the PEM fuel cell. The electrical impedance of the materials used to construct the PEM cell was not considered.

The energy balance of the PEM cell can be formulated by the following equation:

$$\dot{Q}_{net} = \dot{Q}_{chem} - P - \dot{Q}_{uj} - \dot{Q}_{str}, \quad (13)$$

where $\dot{Q}$ is the heat flux, P is the electrical power. Subscript *net* refers to the total heat balance, *chem* to the chemical reaction, *uj* to the latent and sensible heat, and *str* to the acquired stream.

The heat generated by hydrogen consumption in the PEM cell can be described by the equation:

$$\dot{Q}_{chem} = \dot{n}_{\mathrm{H_2}} \Delta H, \quad (14)$$

where $\dot{n}_{H_2}$ is the molar concentration of the reacted hydrogen and ΔH represents the overall enthalpy change during the chemical reaction.

The electrical power generated in the PEM cell is dependent on voltage and current, according to:

$$P = UI, \quad (15)$$

where I is an electric current and U stands for voltage.

The latent and sensible heat depends on the molar energy fluxes of the individual components (hydrogen (H_2), oxygen (O_2), and water (H_2O)) involved in reactions within the PEM cell, as well as the gas-liquid phase transitions that occur, and is expressed by:

$$\begin{aligned}\dot{Q}_{uj} = &\dot{n}_{\mathrm{H_2},out} c_{\mathrm{H_2}} (T - T_o) + \dot{n}_{\mathrm{O_2},out} c_{\mathrm{O_2}} (T - T_o) + \\ &+ \dot{n}_{\mathrm{H_2O}} c_{\mathrm{H_2O}} (T - T_o) + \dot{n}_{\mathrm{H_2O}} (h_S - h_l)\end{aligned}, \quad (16)$$

where: $\dot{n}$ – molar flow rate of a substance, h_s – molar enthalpy of water steam, J/mol; h_l – molar enthalpy of liquid water, J/mol; c_i (i = H_2, O_2, H_2O) – molar specific heat.

The heat transferred from the fuel cell to the heating system is connected to the rate of heat transfer (k), the surface area for heat exchange, and the logarithmic temperature difference (ΔT_{log}), according to equations:

$$\dot{Q}_{str} = A_{PEM} k_{PEM} \frac{(T_{PEM} - T_{wout,PEM}) - (T_{PEM} - T_{win,PEM})}{\ln\left(\frac{(T_{PEM} - T_{wout,PEM})}{(T_{PEM} - T_{win,PEM})}\right)}, \quad (17)$$

$$\dot{Q}_{str} = A_h k_h \frac{(T_{win,h} - T_h) - (T_{wout,h} - T_h)}{\ln\left(\frac{(T_{win,h} - T_h)}{(T_{wout,h} - T_h)}\right)}, \quad (18)$$

Additionally, the transferred heat is defined by the energy balance:

$$\begin{aligned}\dot{Q}_{str} &= \rho w c S\left(T_{win,h} - T_{wout,h}\right) = \\ &= \rho w c S\left(T_{wout,PEM} - T_{win,PEM}\right).\end{aligned} \quad (19)$$

During transient conditions, the term $\dot{Q}_{net}$ representing the change in dynamic heat flux is variable. Under steady conditions $\dot{Q}_{net}$=0. Since the computations were carried out considering transient conditions, the dynamic heat flux is related to the mass of the PEM cell, its overall specific heat, and the temporal temperature change, following the equation:

$$\dot{Q}_{net} = mc \frac{dT}{dt}. \quad (20)$$

The model equations were formulated within the SIMULINK software environment. In the context of the PEM cell, the input parameters were selected to match the parameters reported in [1].

3. Determination of dynamic parameters for building and the PEM fuel cell

3.1. Calculation results for the PEM cell

While examining the fuel cell, its operation was simulated in scenarios both with and without negative feedback. The PID controller (Fig. 1) was incorporated within the negative feedback loop (Fig. 2). Given that the water temperature leaving the fuel cell must remain above 320 K for the underfloor heating system, the logarithmic temperature difference was identified as the analysed state parameter within the negative feedback loop. The flowchart outlining the equations describing the PEM cell model is presented in Fig. 3, and Fig. 4 displays the chart of the PID continuous control system within the negative feedback loop.

The regulatory system of the PEM cell model encompasses an output variable, *Tout*, along with two input variables. These inputs are managed utilising the output signal from the PID system – the molar stream $\dot{n}_{\mathrm{H_2}}$ and the molar stream $\dot{n}_{\mathrm{O_2}}$.

The process of linearizing the open feedback loop system was conducted for a MISO (multi-input, single-output) configuration. This was carried out with the purpose of evaluating the stability of the cell model's response to variations in hydrogen and oxygen supply caused by logarithmic temperature fluctuations. The outcomes of the linearization procedure for the input variable $\dot{n}_{\mathrm{H_2}}$, and the output variable ΔT_{log} of the control object defined as:

$$\Delta T_{log} = \frac{(T_{PEM} - T_{wout,PEM}) - (T_{PEM} - T_{win,PEM})}{\ln\left(\frac{(T_{PEM} - T_{wout,PEM})}{(T_{PEM} - T_{win,PEM})}\right)}, \quad (21)$$

is exhibited in the form of a transfer function:

$$G_{\dot{n}_{H_2}}(s) = \frac{-0.0001512}{s + 0.002122}, \quad (22)$$

where s stands for the Laplace operator.

Similarly, the outcomes of linearizing the control system with respect to the input molar oxygen flow rate ($\dot{n}_{\mathrm{O_2}}$) and the same ΔT_{log} (Eq. (21)) as an output variable, is expressed in the form of a transfer function:

$$G_{\dot{n}_{O_2}}(s) = \frac{-0.00007748}{s + 0.002122}. \quad (23)$$

Linearization of the closed-loop feedback system was carried out, employing the fuel cell's setpoint temperature as the input variable and the fuel cell's logarithmic temperature differ-

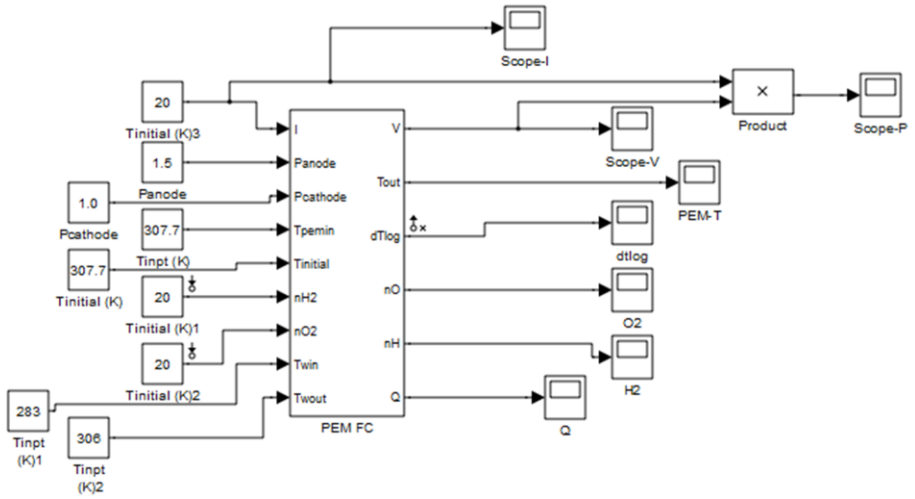

Fig. 3. The flowchart depicting input and output parameters concerning a PEM fuel cell operating in an open feedback loop configuration, excluding any regulatory mechanisms.

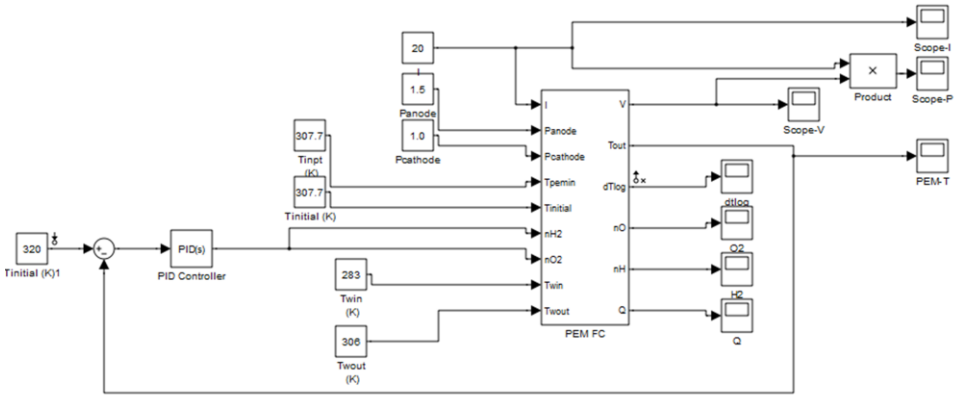

Fig. 4. The flowchart illustrating input and output parameters pertaining to PEM fuel cell with a feedback loop that integrates the PID regulation system.

ence as the output variable. This linearization was specifically applied to a single-input single-output (SISO) object featuring an internal feedback loop responsible for regulating the fuel cell's operating temperature:

$$G_{T_{in}}(s) = \frac{0{,}00005913s + 0{,}0000001578}{s^3 + 0{,}01241s^2 + 0{,}00006092s^2 + 0{,}0000001042}. \quad (24)$$

The behaviour of the closed-loop control system, in conjunction with the designated regulator's setpoint parameters, concerning the stability of the logarithmic temperature difference, is of utmost importance due to its impact on the ability to uphold the thermal characteristics of the simulated building's heating system.

The calculation results for the fuel cell's operation with and without a feedback loop are presented in Figs. 5–7. Figure 5 illustrates the power produced by the fuel cell, while Fig. 6 displays the voltage generated within the fuel cell.

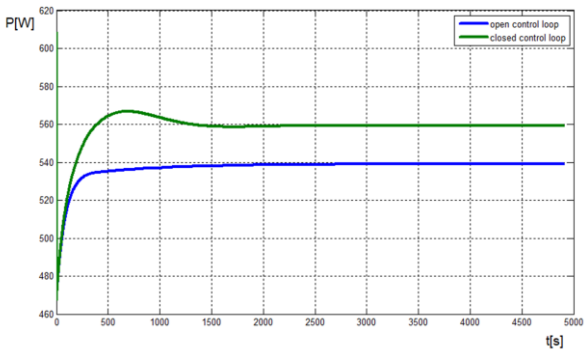

Fig. 5. The power output of the PEM fuel cell under open and closed-loop feedback conditions.

In Figs. 5 and 6, two responses can be observed, where both power and voltage exhibit a more flattened characteristic in the case of an open feedback loop. For the feedback loop, overshooting occurs due to the regulation process involving the mass flow rate of individual streams feeding the PEM cell.

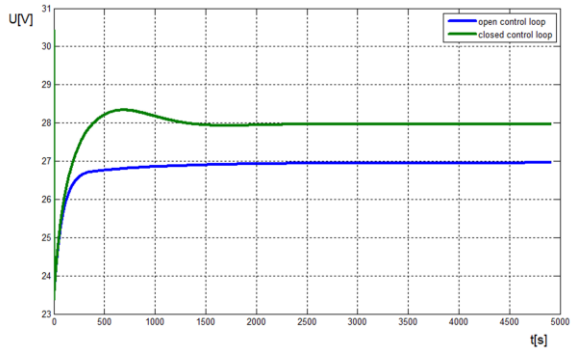

Fig. 6. Voltage on the PEM fuel cell during open and closed-loop feedback operation.

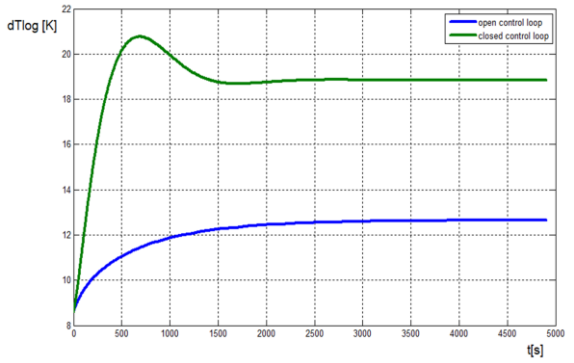

Fig. 7. The logarithmic temperature difference of the PEM fuel cell during operation within an open and closed feedback loop.

Figure 7 depicts the logarithmic temperature difference, which is significant for the heating system of a building.

Furthermore, Fig. 8 provides a graphical representation of the heat generated by the fuel cell, and Fig. 9 exhibits the temperature of the liquid leaving the fuel cell. As it can be seen, the

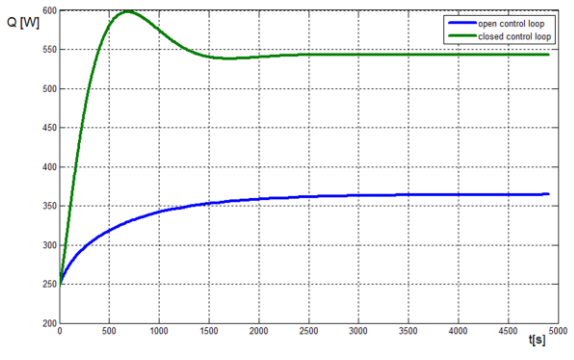

Fig. 8. The heat flow directed to the cooling water during operation within an open and closed feedback loop.

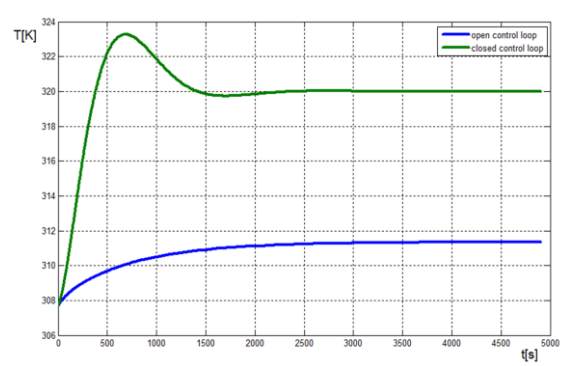

Fig. 9. The operational temperature of the PEM fuel cell during operation within an open and closed feedback loop.

fuel cell temperature increases abruptly in response to the chemical processes occurring in the fuel cell. The results of calculations for the molar oxygen and hydrogen flow rates are shown in Figs. 10 and 11, respectively. They indicate that the molar flow rates of reactants supplied over time cause an overshoot of the fuel cell temperature above the setpoint. Once the temperature exceeds the setpoint (320 K), the molar flowrates are stabilized, resulting in maintaining both thermal and electrical power at a higher level.

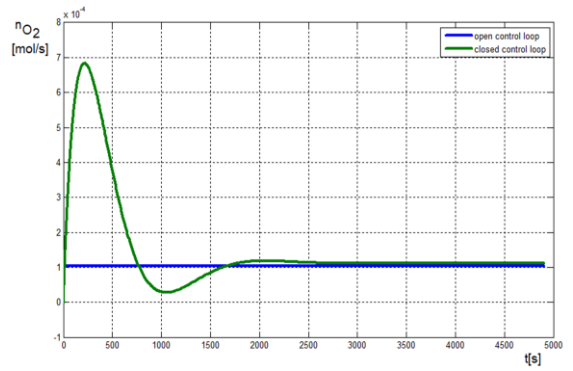

Fig. 10. The molar oxygen flow rate during operation within an open and closed feedback loop.

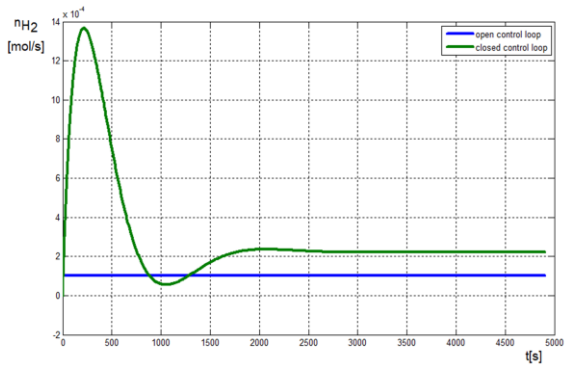

Fig. 11. The molar hydrogen flow rate during operation within an open and closed feedback loop.

In the case of implementing a feedback loop associated with maintaining the outlet temperature of the PEM cell at a specified useful level in the space heating process, an increase in the logarithmic temperature difference is observed (Fig. 7) as well as an increase in the thermal power of the fuel cell (Fig. 8).

Figures from 4 to 9 depict a slight over-regulation of the fuel cell's parameters associated with the regulator's operation, from which the control signals are transmitted to the actuator systems (supply valves). As a result, it becomes essential that the actuator systems (valves) facilitate a wide range of molar flow rates, as illustrated in Fig. 10 and Fig. 11. The molar flow rate experiences a sevenfold increase during transient conditions compared to steady conditions, which corresponds to the initial phases of the fuel cell's chemical reactions. During the initial period, the actuator systems should enable achieving significantly high molar flow rates for both the fuel and the oxidant. Failure of the actuator systems to provide adequately high molar flow rates of reaction substrates could potentially extend the startup time and the duration required to attain the conditions required by the heating systems. For this PEM cell, the elongation of this time could range from 2500 to 4000 seconds.

Figure 12 presents the control error values before processing the signal in the PID controller and the output signal from this controller, whereas Fig. 13 displays the Bode plots, showing both the amplitude and phase characteristics of the controlled system within the closed feedback loop. Upon scrutinizing the Bode plots constructed for the PEM cell control system (Fig. 13), it can be inferred that the system remains stable across the entire amplitude spectrum and exhibits a notably substantial phase margin (approximately 90 degrees).

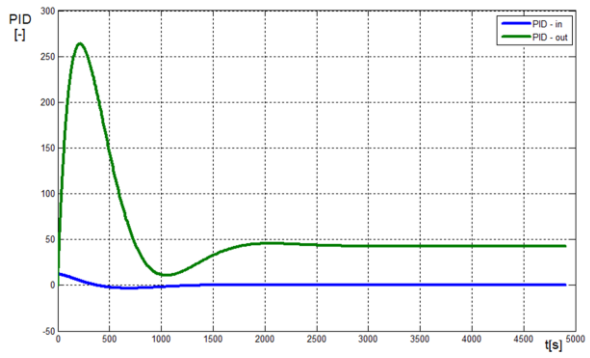

Fig. 12. The control signals at the input and output of the PID regulator.

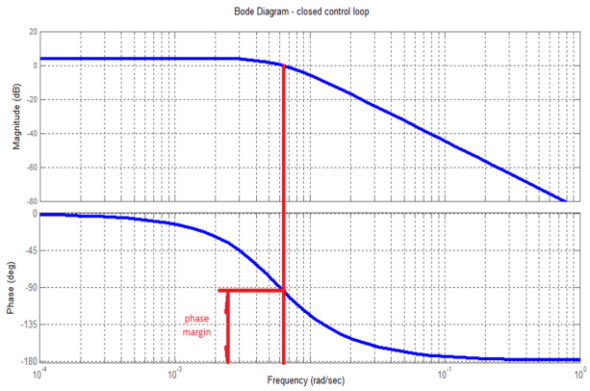

Fig. 13. The Bode plots of the PEM cell system with a closed feedback loop.

2.2. Transient analysis of a building heated by the PEM cell

The investigation involved calculations for determining the thermodynamics of a building heated by a PEM cell. Figure 14 illustrates the signal connections among the PEM cell model, the heating system, and the building, all designed within the SIMULINK software.

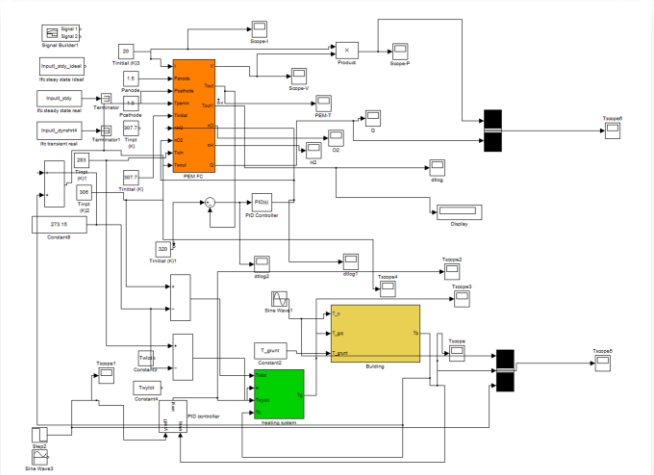

Fig. 14. Implementation of the simulated building heated by the PEM cell, developed in SIMULINK software.

Figure 15 demonstrates variations in the logarithmic temperature difference between the PEM cell and the heating system within heated rooms. The predicted variations of ambient temperature, heated room temperature, and the setpoint temperature of the regulatory system are displayed in Fig. 16. Figure 17 exhibits fluctuations in the operating temperature of the PEM cell. Figure 18 portrays the heat supplied to the heated room (Q) and the electric power produced by the PEM cell (P).

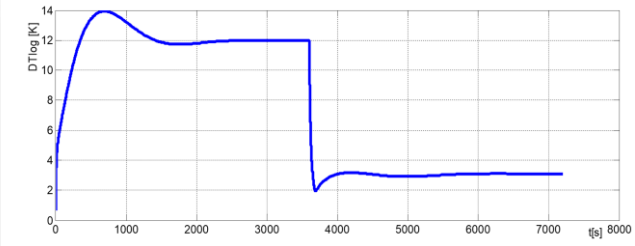

Fig. 15. The logarithmic temperature difference between the PEM cell and the heated water.

Based on the conducted calculations, it is evident that unheated rooms, such as adjacent halls without heating, exert a notable influence on heat losses from the heated rooms. This effect is primarily due to the lack of insulation in the separating walls

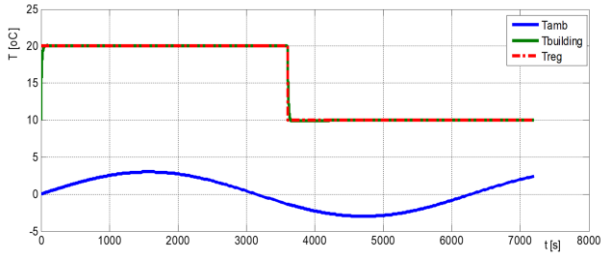

Fig. 16. Ambient temperature, the heated building's temperature and the regulator's setpoint.

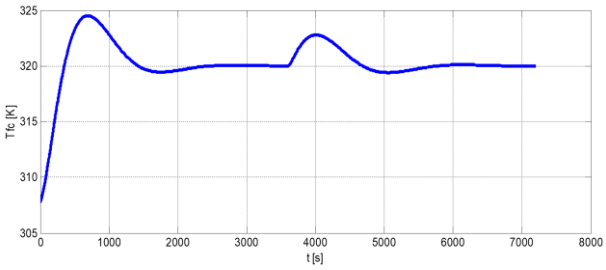

Fig. 17. The operating temperature of the fuel cell.

and the inherent lack of airtightness in front doors and windows in stairwells. Heating of these halls, coupled with ventilation-related losses, can significantly perturb a building's energy balance, subsequently leading to escalated operating costs for the heating system. Addressing this concern, enhancing insulation within the halls becomes imperative.

This situation is especially evident in Fig. 5, where the temperature rise in the halls contiguous to the heated rooms occurs at a relatively gradual pace. This behaviour is attributed to the interplay of ambient temperature and the heat transfer coefficient of the non-insulated walls. The oscillation in ambient temperature T_o (variation between approximately –3°C and +3°C as in Fig. 16) is attenuated due to heat penetration through the walls, having minimal effect on room temperatures. The minor temperature fluctuations (Fig. 17), arising from the operation of the thermostatic valve within the building's heating system, are mitigated by the mass flow rate of heating water obtained from the PEM fuel cell via the PID regulator, as described by Eq. (10). Consequently, the fuel cell maintains stable thermal parameters for the cooling system. As a result, the heat derived from the PEM fuel cell also remains stable.

Discussing the potential use of waste heat from fuel cells for heating purposes is intriguing, yet it requires in-depth analysis. Understanding the heat transfer processes from cells to the building's heating system and the technical aspects of integrating these two systems are pivotal. Optimal utilisation of waste heat can significantly amplify the overall energy efficiency of the system.

One crucial aspect worth highlighting is the efficiency of proton exchange membranes (PEM) in fuel cells. This membrane plays a pivotal role by enabling the flow of protons between the anode and cathode, thereby generating electric current. However, in practice, the effectiveness of PEMs can be hindered by factors such as humidity, temperature, and the presence of impurities. Hence, continuous research into refining membrane technology is essential to ensure reliability and efficiency.

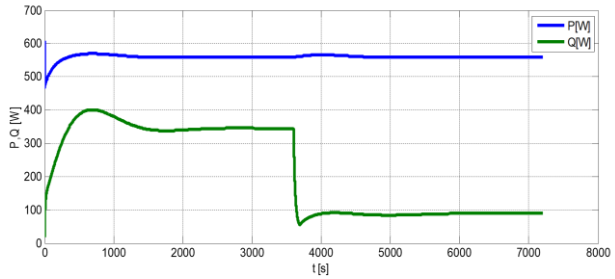

Fig. 18. The thermal power (Q) employed for heating purposes and the electrical power (P) produced by the PEM cell.

3. Conclusions

In the realm of cutting-edge building technology, this work presents a pioneering exploration in the field of sustainable thermal management by integrating Proton Exchange Membrane (PEM) fuel cells into the heating systems of modern structures. At its core, this investigation pivots on the innovative utilisation of waste heat emanating from PEM fuel cells, repurposing it as a strategic asset to foster a more energy-efficient and sustainable approach to building heating.

The cornerstone of this research lies in the development and presentation of a robust mathematical model. This model serves as a sophisticated analytical tool, meticulously mapping out the intricate interactions between the thermal dynamics inherent to PEM fuel cells and the variable heating demands typical of contemporary buildings. This is particularly emphasized under transient operational conditions, a crucial factor in optimizing the system's overall performance.

A focal point of the study is the operational parameters of the PEM cells. When situated within a closed feedback loop, these cells exhibit an operating temperature orbiting around 320 K. This is contrasted with their performance in an open feedback loop, where the temperature is capped at a slightly lower threshold of 312 K. The research underscores the efficacy of a regulatory system capable of modulating the molar flow rates of hydrogen and oxygen, adjusting them to the stoichiometric amounts required for the cell's chemical reactions. The ingenuity of this system lies in its dual-regulation capability, allowing for controlling both oxygen and hydrogen molar flow rates with precision.

When the PEM cell is configured to function as a cogeneration unit, the study reveals its capacity to achieve optimal cooling water thermal parameters. This facilitates the concurrent generation of both heat and electrical power, a testament to the cell's versatility and efficiency. Theoretical analyses deduce that the thermal inertia of adjoining unheated rooms plays a significant role in the overall thermal balance, mainly governed by the

heat transfer coefficients, and the physical characteristics of the walls.

The research highlights the stabilizing role of the proportional-integral-derivative (PID) regulator in maintaining the cooling water supply to the fuel cell. This regulator effectively mitigates minor fluctuations induced by the building's heating system thermostat, ensuring consistent operational conditions.

The paper further delves into the thermal implications of unheated rooms on the overall heat loss in heated spaces, advocating for the strategic insulation of these areas. This insight holds particular relevance for older buildings that may lack modern insulation standards, suggesting potential retrofitting solutions to enhance their energy efficiency.

In conclusion, this work not only charts new territory in the field of building heating systems but also sets forth a comprehensive roadmap for future research. It calls for an in-depth exploration into areas such as membrane efficiency, advanced control strategies, and the integration of renewable energy sources. This forward-thinking perspective holds the promise of harnessing the full potential of PEM fuel cell technology, potentially leadinga transformative shift in the landscape of heating technology.

References

[1] Nehrir, M., & Wang, C. (2009). *Modeling and control of fuel cells*. IEEE Press, John Wiley & Sons, Inc.

[2] Spiegel, C. (2008). *PEM fuel cell modeling and simulation using MATLAB*. Academic Press.

[3] Abdin, Z., Webb, M. C., & Gray, A. (2016). PEM fuel cell model and simulation in MATLAB/Simulink based on physical parameters. *Energy*, 116, 1131–1144. doi: 10.1016/j.energy.2016.05.096

[4] Taner, T. (2018). Energy and exergy analyze of PEM fuel cell: A case study of modeling and simulations. *Energy*, 143, 284–294. doi: 10.1016/j.energy.2017.10.102

[5] Taner, T. (2021). The novel and innovative design with using H2 fuel of PEM fuel cell: Efficiency of thermodynamic analyze. *Fuel*, 302, 121109. doi: 10.1016/j.fuel.2021.121109

[6] Naqvi, S.A.H., Taner, T., Ozkaymak, M., & Hafiz, M.A. (2022). Hydrogen production through alkaline electrolyzers: A techno-economic and enviro-economic analysis. *Chemical Engineering and Technology*, 46(3), 474–481. doi: 10.1002/ceat.202200234

[7] Taner, T., Naqvi, S.A.H., & Ozkaymak, M. (2019). Techno-economic analysis of a more efficient hydrogen generation system prototype: A case study of PEM electrolyzer with Cr-C coated SS304 bipolar plates. *Fuel Cells*. doi: 10.1002/fuce.201700225

[8] Sudarshan, L.C., & Dhananjay, T.B. (2017). Modeling and performance evaluation of PEM fuel cell by controlling its input parameters. *Energy*, 138, 437–445. doi: 10.1016/j.energy.2017.07.063

[9] Mingruo, H., Anzhong, G., Minghua, W., Xinjian, Z., & Lijun, Y. (2004). Three dimensional, two phase flow mathematical model for PEM fuel cell: Part I. Model development. *Energy Conversion and Management*, 45, 1861–1882. doi: 10.1016/j.enconman.2003.09.009

[10] Ziogou, C., Voutetakis, S., Papadopoulou, S., & Georgiadis, M.C. (2011). Modeling, simulation and experimental validation of a PEM fuel cell system. *Computers and Chemical Engineering*, 35, 1886–1900. doi: 10.1016/j.compchemeng.2010.11.018

[11] Vida, M., & Gholamreza, K. (2012). Dynamic modeling, optimization and control of power density in a PEM fuel cell. *Applied Energy*, 93, 98–105. doi: 10.1016/j.apenergy.2011.12.067

[12] Waseem, S., & Ghait, W. (2015). Modeling and analysis of renewable PEM fuel cell system. In *International Conference on Technologies and Materials for Renewable Energy, Environment and Sustainability, TMREES15*. *Energy Procedia*, 74, 87–101. doi: 10.1016/j.egypro.2015.07.506

[13] Horng-We, W. (2016). A review of recent development: Transport and performance modeling of PEM fuel cells. *Applied Energy*, 165, 81–1062. doi: 10.1016/j.apenergy.2015.12.011

[14] MathWorks. (n.d.). *Simscape Electrical*. https://uk.mathworks.com/products/simscape-electrical.html [accessed 1 Sept. 2023]

[15] Capizzi, G., Sciuto, G.L., Cammarata, G., & Cammarata, M. (2017). Thermal transients simulations of a building by a dynamic model based on thermal-electrical analogy: Evaluation and implementation issue. *Applied Energy*, 199, 323–334. doi: 10.1016/j.apenergy.2017.05.099

[16] Mikielewicz, J. (1995). *Modeling of thermal and flow processes*. Maszyny Przepływowe, vol. 17, Ossolineum, Wrocław (in Polish).

[17] Charun, H. (2005). *Fundamentals of energy management. Part 2, Examples of application*. Wydawnictwo Politechniki Koszalińskiej, Koszalin (in Polish).

[18] Song, B., Bai, L., & Yang, L. (2022). Analysis of the long-term effects of solar radiation on the indoor thermal comfort in office buildings. *Energy*, 247, 123–499. doi: 10.1016/j.energy.2022.123499

[19] Wonorahardjo, S., Sutjahja, I., Mardiyati, Y., Andoni, H., Achsani, A.R., Steven, S., Dixon, T., Ekrem, T., Müslüm, A., & Rahmah, N. (2022). Effect of different building façade systems on thermal comfort and urban heat island phenomenon: An experimental analysis. *Building and Environment*, 217(12b), 109063. doi: 10.1016/j.buildenv.2022.109063

[20] Wu, J., Li, X., Yang, L., Yan, Y., & Tu, J. (2020). A PMV-based HVAC control strategy for office rooms subjected to solar radiation. *Building and Environment*, 177, 106–863. doi: 10.1016/j.buildenv.2020.106863

[21] Mao, N., Hao, J., He, T., Song, M., Xu, Y., & Deng, S. (2019). PMV-based dynamic optimization of energy consumption for a residential task/ambient air conditioning system in different climate zones. *Renewable Energy*, 142, 41–54. doi: 10.1016/j.renene.2019.04.118

[22] Buyak, N., Bilous, I., Pavlenko, A., Sapunov, A., Biriukov, D., & Dashenko, V. (2023). Dynamic interdependence of comfortable thermal conditions and energy efficiency increase in a nursery school building for heating and cooling period. *Energy*, 283, 129076. doi: 10.1016/j.energy.2023.122195

[23] Matysko, R., & Dyczkowska, M. (2018). Thermal dynamics of a building. *Transactions of the Institute of Fluid-Flow Machinery*, 141, 31–40.